COLOUR CORRECTION FOR ASSESSING PLANT PATHOLOGY USING LOW QUALITY CAMERAS

Sion Hannuna, Timo Kunkel, Nantheera Anantrasirichai and Nishan Canagarajah
Department of Computer Science, University of Bristol, Woodland Road, Bristol, BS8 1UB, U.K.

Keywords: Plants, Pathology, Colour, Characterisation, MacBeth ColorChecker, Mobile phone, Camera.

Abstract: We describe a framework for standardising the colour of plant images taken using both mobile phones and compact cameras. This is with a view to maximising the accuracy of plant pathology diagnosis. Rather than attempt to characterise each camera, we place cheap and easily portable custom colour targets in the scene being captured. We propose a novel weighted least squares formulation for optimising the transformation function deduced for each image, where the relative contribution for each patch is proportional to the number of closely matching pixels in the image to be transformed. We also introduce our custom colour target which has been designed to preferentially map plant colours and facilitate simple automatic extraction from the image being processed. We provide subjective and objective results demonstrating the efficacy of our approach. It is anticipated that the methods described here could be applied to any application where perceptual consistency is of value.

1 INTRODUCTION

The appearance of images depends on various elements. On the acquisition side, it is influenced by the interaction of the scene's content, the lighting conditions and the capture device. On the display side it is affected by the screen set-up and its local environment with both influencing how the human visual system perceives the scene (Fairchild, 2005). For example the same image will look different under artificial and natural lighting. Note that these perceptual differences are not just a byproduct of the HVS: the actual pixel values of the same object are highly dependent on capture conditions. This makes the use of colour and intensity information as features for automatic analysis very problematic.

One way of addressing the issues originating on the capture side is by using a fully characterised camera under controlled lighting coupled with a monitor calibrated to the ambient lighting of the user's environment (Fairchild, 2005). This is not always feasible in applications where the capture conditions and exact device properties are not known, for example in rural areas where the use of specialised equipment is difficult or not easily achievable.

This work forms part of a proposed agriculture disease mitigation system which aims to provide a mobile phone based 'Farmer to Expert' service, which facilitates prompt access to disease and pest mitigation advice. In order to enable the expert to provide relevant information, they are provided with data about the farmers' crops. This would include soil type and pH, crop variety and the pesticides and fertilizers being used.

The text-based information available to the expert will be augmented with mobile phone photos of the crops, which have been captured and uploaded by the farmer at the time of advice being sought. Unfortunately, the photos taken will be sensitive to a number of factors including camera type and lighting incident on the scene. Ideally, the images would be processed in such a way as to provide the expert with a visual representation of the affected crops that reflects the true nature of the scene.

In this paper we propose a cheap and easily implemented approximation to such a solution that makes use of automatically detected colour charts facilitating its integration into colour-managed imaging pipelines. The motivation for maximising how realistic the plant images are is that a great deal of information about the plants' health may be gleaned from their colours. Figure 1 shows two red maple leaves afflicted with different mineral deficiencies. Different capture conditions can greatly affect how those images appear. In addition to striving for perceptual consistency, objective colour consistency increases the

Hannuna S., Kunkel T., Anantrasirichai N. and Canagarajah N..
COLOUR CORRECTION FOR ASSESSING PLANT PATHOLOGY USING LOW QUALITY CAMERAS.
DOI: 10.5220/0003291303260331
In *Proceedings of the International Conference on Bioinformatics Models, Methods and Algorithms* (BIOINFORMATICS-2011), pages 326-331
ISBN: 978-989-8425-36-2

(a) (b)

Figure 1: Iron (*a*) and magnesium (*b*) deficiency in red maple (*Acer rubrum L.*). Images by John Ruter, University of Georgia, Bugwood.org.

potential for fully exploiting colour as a feature in automated systems.

2 STANDARDISING FOR LIGHTING AND CAMERA VARIATION

Recall that the aim of our system is to standardise images from low quality cameras such that they are both consistent with one another and provide a faithful representation of the scene they depict. To facilitate both subjective and objective assessment of the efficacy of the algorithms described here, the photos taken by a Canon EOS 5D mkII DSLR camera are assumed to reflect the truest representation of the scene and provide a ground truth / target for the output from the other cameras used: in a 'live' setup colour chart values measured under standardised lighting would be used to deduce the necessary transformation.

2.1 Colour Chart Specification

In order to obtain an independent measure of the colour in an image, colour targets are placed in the scene which is to be captured. A common target widely used in colorimetry and photography is the X-Rite (former Gretag-MacBeth) ColorChecker. In our experiments we employ both this target and one of our own devising that has been tailored to our needs. Specifically, a white border has been added to facilitate automatic detection and 'greenish' colours have been more numerously represented. It was anticipated that by more heavily weighting areas of the gamut where foliage colours generally reside, they may be more accurately transformed.

As the longer term objective of this work involves deployment in rural India, the replication cost of the colour targets has to be low. This is achieved by using a traditional chemical printing process creating costs of less than 10 cents per target. To avoid specular highlights in the colour target, it is printed on matte photo-paper. A further design decision was to print the target in credit-card size. This enables the farmer to have the target at hand when needed.

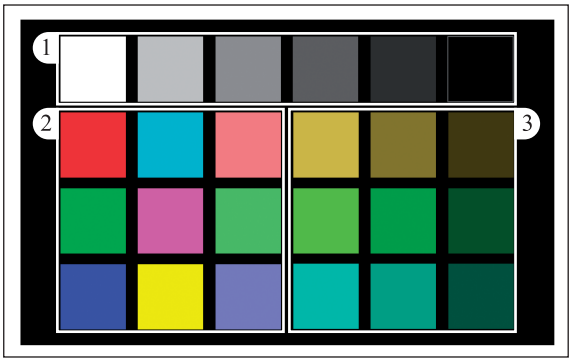

Figure 2: Custom colour target designed to preferentially map plant colours and enable automatic segmentation. Note that the white numbered boxes in the figure are for illustration purposes only and not part of our implemented target.

The custom target shown in Figure 2 offers three groups of colour patches. Group 1 is composed of achromatic colours (from white to black in 20% steps). Group 2 includes primary (RGB in 100% and 50% opacity) as well as secondary colours (CMY). The last group, 3, contains green tones created in CIE $L^*a^*b^*$ colour space with L^* values of 25, 50 and 75 as well as a^* and b^* set to -65/65, -65/0 and 0/65. Note that our custom chart, like the X-Rite ColorChecker Passport, has only 24 patches. The colour charts generally used in device characterisation, usually contain more patches (e.g. the ColorChecker DC has 192). Whilst this increases the potential for generalisation, the detection accuracy of the individual patches on a credit-card sized target will decrease with an increasing number of patches.

2.2 Colour Chart Extraction

Whilst the X-Rite colour target is hand segmented by labeling its four corners, the custom colour chart is automatically segmented by exploiting the white border surrounding the black background to the patches. Specifically, the images are converted to greyscale and the contrast is maximised. These are then thresholded to produce binary images to which a Canny edge detector is applied. By considering the intersection point of perpendicular edges in conjunction with the processed greyscale image, it is possible to segment the chart's border and hence the patches within. Finally the difference between the values of the detected colours and the expected colours is calculated. The colour chart is correctly detected if the difference value is within acceptable variation.

2.3 Deducing a Transformation Matrix

The patch values for the source image to be processed and the ground truth image taken by the DSLR are used to deduce a transformation for the source image. This process is analogous to the characterisation of imaging devices including digital cameras. Various characterisation methods exist (Luo and Rhodes, 2001; Tominaga, 1999). They essentially involve deducing a mapping for targets that have known device independent CIE XYZ values. Linear and polynomial transformations have been used to this end as well as neural networks. However, an important distinction for our application should be noted: normally characterisation is done *once for a given device*. Hence it is important that the mapping used generalises for all conceivable scenes and lighting conditions. Conversely, in our application, we only need the mapping to work well for one particular image.

To exploit this stipulation we have experimented with weighting the relative cost for the residual error of particular patches under the deduced transformation according to how numerous image pixels closest to that patch are in a given image. Hence, in most of our images greens and browns would be favoured as they primarily depict plants. For the quadratic and linear transformations we utilise, this lends itself to a weighted least squares optimisation. We term this our 'heuristic' approach, whereas normal least squares will hereafter be referred to as 'pure'.

The colour targets we tested only have 24 patches. We found this was not enough correspondences for training MLP neural networks and Support Vector Machines as generalisation was poor. Conversely, the quadratic and linear transformations considered here produce perceptually convincing results. Cheung and Westland describe a quadratic mapping function (Cheung and Westland, 2002) formulation that may be solved as a linear system (see Equation 1):

$$\begin{aligned} X &= a_1R + a_2G + a_3B \\ &+ a_4RG + a_5RB + a_6GB \\ &+ a_7R^2 + a_8G^2 + a_9B^2 + a_{10} \\ Y &= a_{11}R + a_{12}G + a_{13}B \\ &+ a_{14}RG + a_{15}RB + a_{16}GB \\ &+ a_{17}R^2 + a_{18}G^2 + a_{19}B^2 + a_{20} \\ Z &= a_{21}R + a_{22}G + a_{23}B \\ &+ a_{24}RG + a_{25}RB + a_{26}GB \\ &+ a_{27}R^2 + a_{28}G^2 + a_{29}B^2 + a_{30} \end{aligned} \quad (1)$$

We experimented with this formulation as well, as a basic linear transformation shown in Equation 2 and a simplified version of the polynomial described in Equation 1. where the constant and interaction terms for the tristimulus values were dropped as given in Equation 3.

$$\begin{aligned} X &= a_1R + a_2G + a_3B \\ Y &= a_4R + a_4G + a_6B \\ Z &= a_7R + a_8G + a_9B \end{aligned} \quad (2)$$

$$\begin{aligned} X &= a_1R + a_2G + a_3B \\ &+ a_4R^2 + a_5G^2 + a_6B^2 \\ Y &= a_7R + a_8G + a_9B \\ &+ a_{10}R^2 + a_{11}G^2 + a_{12}B^2 \\ Z &= a_{13}R + a_{14}G + a_{15}B \\ &+ a_{16}R^2 + a_{17}G^2 + a_{18}B^2 \end{aligned} \quad (3)$$

For each of the colour charts, the above formulations were tested using both least squares optimisation ('pure') and weighted least squares based on the content of the image being processed ('heuristic'). Specifically for each pixel the Euclidian distance from every patch was determined. Each patch's weighting was based upon the total number of pixels that were closest to it in the camera's device dependent RGB colour space. This process is analogous to preselecting colour patch values on the basis of the application area. Cheung and Westland (Cheung and Westland, 2004) note that it would be sensible to select a characterization set based on the colour of the object being measured. Our approach is to augment this process by skewing the optimisation such that colours depicted in the image or more heavily favoured.

3 RESULTS AND EVALUATION

Two data sets are presented here. The first were taken at our university botanical gardens in late spring. Fifteen different plants were photographed with 5 different cameras including the DLSR which acts as our ground truth. Generally 2-3 shots were taken with each camera to ensure at least one of acceptable quality would be available. Objective results and sample images are provided below. Analysis was performed using the X-Rite ColorChecker. Results for the polynomial function defined in Equation 1 were relatively poor in comparison and thus are not presented here. This may be as 24 samples were inadequate to train a function of this complexity as others have reported that 40 to 60 are a suitable number (Luo and Rhodes, 2001).

The second data set trials our custom colour chart and compares it's effectiveness against the ColorChecker chart in out application. Once again 5 cameras were used including the DSLR. In these photos, collections of leaves from different plants were used.

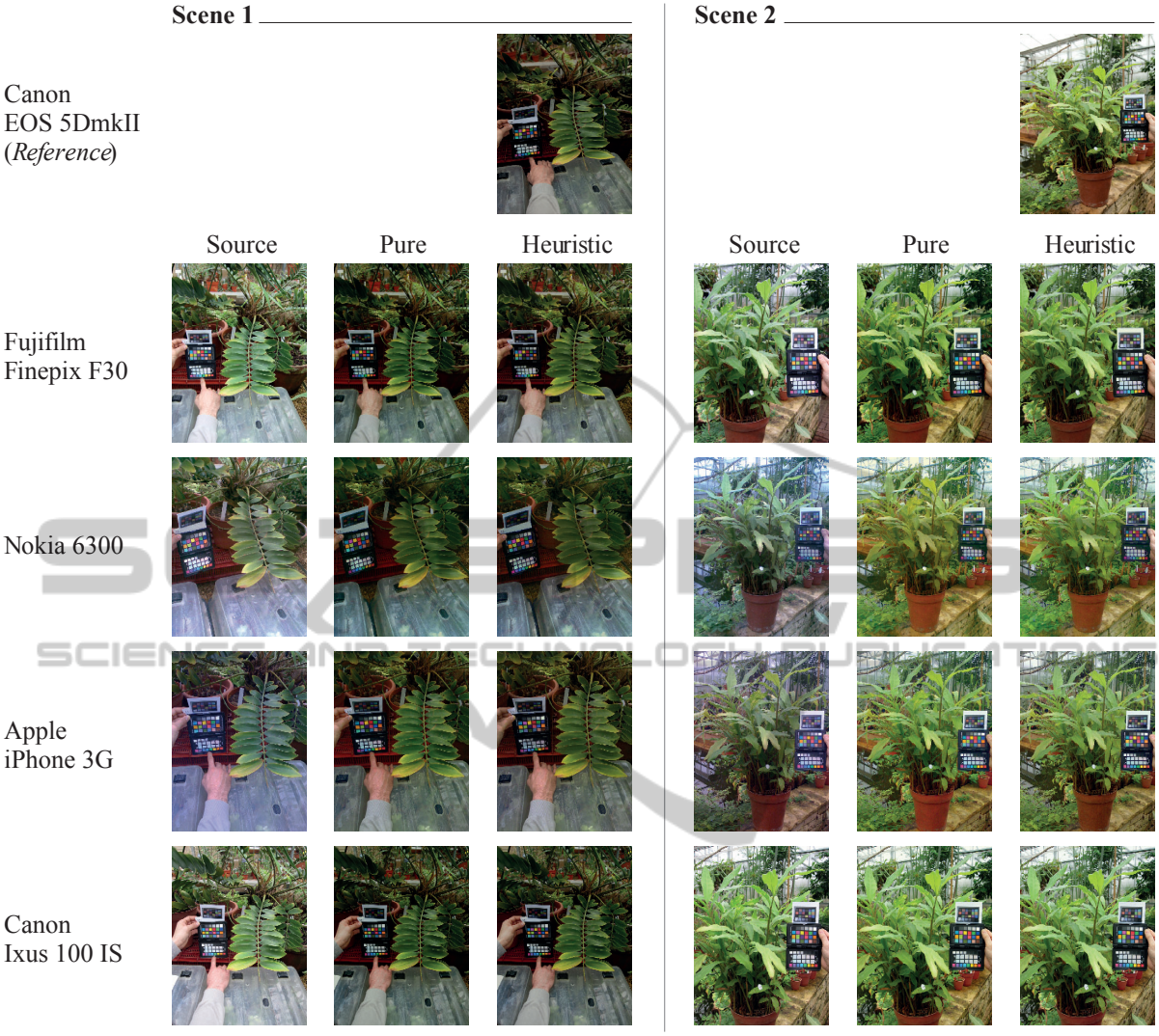

Figure 3: Sample scenes visually demonstrating relative efficacy of our methodology.

Example results for our algorithms for both the botanical gardens and the scene containing sample leaves are provided in Figures 3 and 4 respectively. In each figure source and destination images are contrasted against the simplified quadratic transformation with and without the use of weighted least squares. Note that the transformed images look more similar to the target than the source image. The images in Figure 4 were processed using our custom chart, whereas those in Figure 3 utilised the ColorChecker.

To obtain an objective measure of similarity we follow Rubner et al.'s approach (Rubner et al., 1998) to assessing the distance between the transformed images and the target. Note that as the images are taken form different viewpoints it is not possible to perform a pixel-wise comparison.

Rubner et al. (Rubner et al., 1998) demonstrate that their Earth Mover's Distance (EMD) metric used in conjunction with images transformed into CIE-LAB colour space effectively clusters perceptually similar images and hence is employed here. Global CIE-LAB colour histograms for the target, source, and transformed images were generated using 10 bins per channel. The EMD was calculated for the latter three images with respect to the target image. Note that as the target image is taken from a slightly different perspective to the others, one would not expect even 'perceptually perfect' correspondences to yield a zero EMD.

Figure 6 summarises the EMD results for out transformations compared against the EMD for the source image. In all cases the images are significantly 'closer' to the target after being transformed. For the botanical gardens' images the simplified quadratic

formulation outperforms the linear transform for the Fujifilm Finepix F30 and the Apple iPhone 3G, whereas the linear transform is better for other two cameras. However, both produce faithful results and these numbers are in good agreement with our experience of eyeballing the images.

Encouragingly, the custom target performs, in general, as well as the ColorChecker, indeed it works better for the Nokia 6300 images in the limited test we performed. Furthermore, our approach using weighted least squares optimisation, generally performs slightly better than using the standard least squares approach.

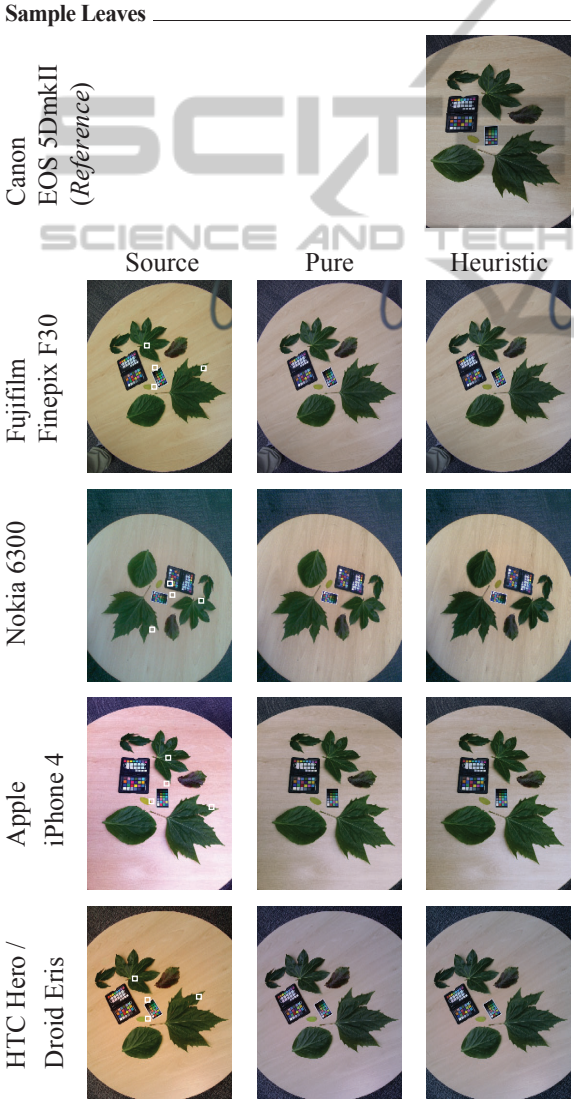

Figure 4: Scene visually demonstrating relative efficacy of our methodology. The white rectangles in the source images represent the sample patches used to compute the ΔE values 25 to 28 in Figure 5.

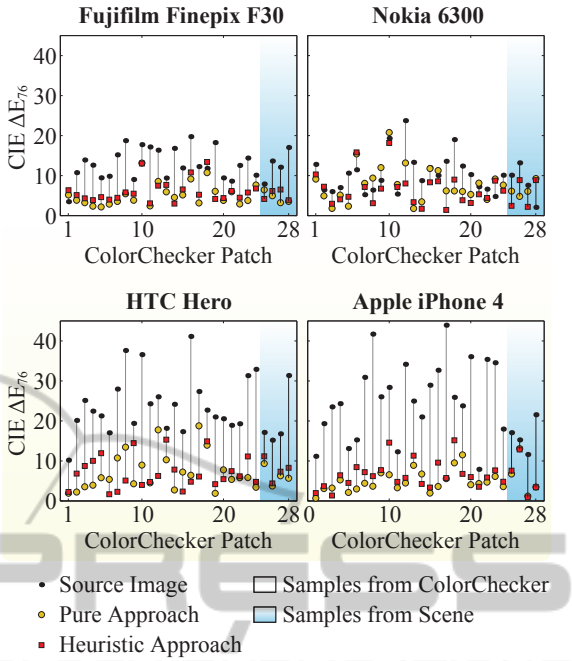

Figure 5: The colour difference for all four cameras. The numbers on the abscissa represent the standard ColorChecker patches (left to right, top to bottom, starting with black patch). Further, patch number 25 to 28 represent measurements in the scene shown in Figure 4.

For the results depicted in Figure 4, the transformation function was optimised using our custom chart. This enables us to use the ColorChecker target as a test set for calculating the colour differences for its 24 patches. We also analysed four hand selected image regions. In both cases, the CIE ΔE_{76} colour difference metric was used. The results are shown in Figure 5. The colour difference is reduced significantly for all four cameras for both the 'pure' (standard least squares) and 'heuristic' (weighted least squares) approach. CIE ΔE values between 3 and 6 are normally not perceived as different by naive observers. Note that some of the ColorChecker values show a relatively high error (> 10). These are usually colours which are perceptually distant to the 'greenish' values of interest (e.g. the deep red patch 10 and the orange patch 18).

4 DISPLAY

After the colours of the input image have been mapped using our colour target, the photograph can, for example, be converted to the sRGB colour space. In a fully colour-managed imaging pipeline e.g. using ICC-profiles and calibrated display devices, it is now faithfully represented. Alternatively, the percep-

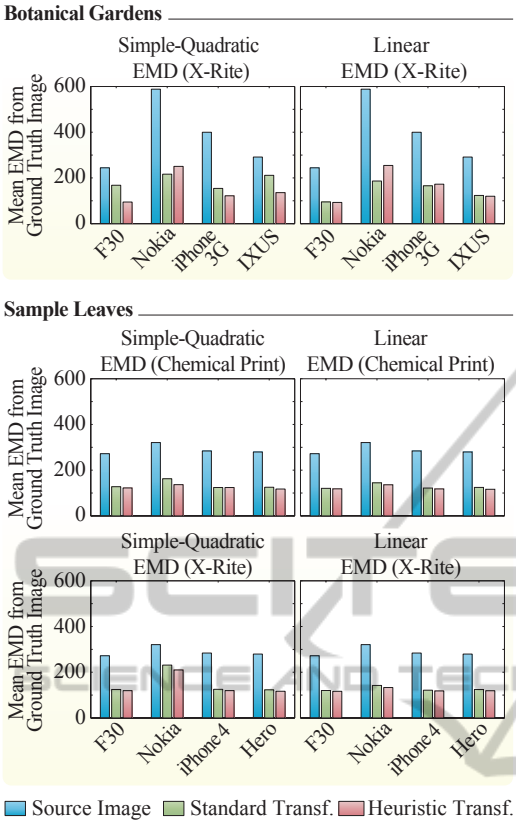

Figure 6: Mean EMD for all image analysed.

tual accuracy of our approach can be further increased by adjusting the photo of the plant to the current state of human visual system. This can be achieved by applying a colour appearance model (CAM), which extends the above imaging pipeline by taking into account the display's environment, before showing the image (Fairchild, 2005).

5 CONCLUSIONS

An approach to standardising plant images for pathology diagnosis has been detailed. The efficacy of our custom colour chart and the use of a weighted least squares formulation has been demonstrated. It is anticipated that the method described here will be applicable to other applications utilising colour images, that cannot be captured in repeatable way, for quality control and assessment purposes. Future work will more rigorously test our approach by applying it to other classes of image. Furthermore, we plan to combine the standardised colour information with other image features to enable automatic classification and diagnosis.

ACKNOWLEDGEMENTS

The authors would like to acknowledge the support of the IU-ATC (http://www.iu-atc.com). We also thank the Bristol University Botanical Gardens.

REFERENCES

Cheung, T. L. V. and Westland, S. (2002). Color camera characterisation using artificial neural networks. *Proceedings of the 10th Color Imaging Conference*, pages 117–120.

Cheung, T. L. V. and Westland, S. (2004). Color selections for characterization charts. *Proceedings of the Second European Conference on Colour in Graphics, Imaging and Vision*, pages 116–119.

Fairchild, M. D. (2005). *Color Appearance Models*. Wiley-IS&T Series in Imaging Science and Technology, 2nd edition.

Luo, M. and Rhodes, P. (2001). A study of digital camera colorimetric characterisation based on polynomial modelling. *Color Research and Application*, 26:76–84.

Rubner, Y., Tomasi, C., and Guibas, L. J. (1998). A metric for distributions with applications to image databases. In *ICCV*, page 59, Washington, DC, USA.

Tominaga, S. (1999). Color coordinate conversion via neural networks. *Colour Imaging: Vision and Technology, ed. Lindsay W. MacDonald and M. Ronnier Luo*, pages 166–178.